ELSEVIER

Physics of the Earth and Planetary Interiors 126 (2001) 195–210

PHYSICS OF THE EARTH AND PLANETARY INTERIORS

www.elsevier.com/locate/pepi

Three-dimensional (3-D) thermal investigation below high Alpine topography

T. Kohl*, S. Signorelli, L. Rybach

Institute of Geophysics, ETH-Hönggerberg, CH-8093 Zürich, Switzerland

Received 27 February 2000; received in revised form 12 October 2000; accepted 1 April 2001

Abstract

The characteristics of severe topography in active mountain belts represent a special challenge for the evaluation of subsurface temperatures. These conditions require in particular a proper treatment of possible thermally relevant mechanisms. In the present analysis temperature data from depths of up to 1.5 km are investigated which have been collected at the intermediate "point-of-attack" in the framework of the new Alpine transverse (NEAT) project in central Switzerland for the construction of a 57 km long base tunnel. Specially designed temperature measurements were used in a 800 m deep shaft and along a 1200 m long access adit. Additional thermal information was provided by temperature logs from two nearby exploration boreholes and from laboratory measurements of various samples.

For a detailed investigation of the temperature data a transient finite element (FE) model has been used which accounts for fluid and mass advection (uplift) as well as for climatic changes. The uplift and exhumation scenario assumed the surface to be in steady-state conditions. Special emphasis was given to structural effects like topography and anisotropy. The 3-D numerical model extends over an area of ~20 km × 20 km and includes Alpine high topographic relief with altitudes between 1500 and 3000 m a.s.l. Without modifying petrophysical parameters determined from laboratory measurements, all reliable temperature data could be nearly perfectly fitted by adjusting the two principal thermal boundary conditions at the surface and at the bottom. This study reveals that hydraulic influence is generally negligible at depths below ~500 m which is in contrast to results from lower-dimensional methods such as 1-D Péclet analyses. Vertical heat flow variations are rather due to topographic than to hydraulic impact. Sensitivity studies highlight the importance of uplift in the central Swiss Alps and of local ground surface temperature (GST) distribution which both can influence the temperature field even at greater depths.

Keywords: Topography; Heat flow; Alpine tectonics; Advection; Uplift/erosion

1. Introduction

The subsurface temperature field in Alpine settings is the result of strongly undulating topographical units, complex geological structures and of physical processes associated with the past and ongoing Alpine tectonics. The exact temperature information in this terrain can be of great importance for construction and operational conditions in deep underground buildings. In this regard rock temperature prediction is of paramount importance for the tunnels currently being constructed in the framework of the new Alpine transverse (NEAT) project in central Switzerland. An accurate prediction of tunnel temperatures at the beginning of the planning phase enables the development of engineering concepts for the dimension of ventilation during construction and operation, and

* Corresponding author. Fax: +41-1633-1065.
E-mail address: kohl@ig.erdw.ethz.ch (T. Kohl).

0031-9201/01/$ – see front matter
PII: S0031-9201(01)00255-2

thus provides long-term financial reliability. More importantly, however, an anomalous temperature can be used as indicator for fluid flow ahead of the tunnel face (Busslinger and Rybach, 1999a). Precise measurements of the ambient temperature field during tunnelling and an accurate thermal model of the specific location are both required. Deviations between predicted and measured temperature allows one to estimate the importance of fluid advection and the distance to water-bearing karstic or fracture zones.

The most essential part of the NEAT project a new 57 km railway tunnel (Gotthard base tunnel) should link the northern and southern part of Switzerland across a number of nearly vertically structured crystalline massifs (i.e. Gotthard and Aar massifs) at an altitude of 550 m. With a maximum depth of overburden of 2500 m, high temperatures have to be expected. Specific zones posing possible geotechnical problems are the tectonically highly deformed Tavetsch massif near the centre of the tunnel and the highly permeable Piora zone in the south of the tunnel. The latter one has already been investigated by an adit completed in 1997 (Busslinger and Rybach, 1999a) whereas the Tavetsch massif is currently being investigated by shaft and adit construction, combined with exploration boreholes near the community of Sedrun. Both shaft and adit will later serve as intermediate "point-of-attack" for the final tunnelling. Shown on the vertical cross-section in Fig. 1 are the proposed tunnel, a 1000 m long access adit from Sedrun, a high chamber for the shaft head, a 450 m long ventilation shaft to the valley Val Nalps on the other side of the mountain range and a 800 m deep vertical shaft which reaches at its bottom part down to the future base tunnel level. From there, at ∼1200 m below surface the tectonically highly deformed Tavetsch massif will be traversed by the Gotthard base tunnel. To further investigate the surrounding rock masses four inclined exploration boreholes (SB1, SB2, SB3.2, and SB4.1) have been drilled in the northern part of the Tavetsch massif (see Fig. 1) with two of them reaching the level of the future base tunnel. Temperature data of different quality are available from adit, shaft and boreholes (see later).

The first temperature predictions for the Gotthard base tunnel were performed by Rybach and Pfister (1994). At that time the calculations assumed pure conductive heat transport and an analytical treatment of 3-D topography. Based on temperature data collected mainly in the south of the future base tunnel but also on thermal conductivity and heat production data of the individual lithological units Busslinger and Rybach (1999b) later improved this model by accounting for fluid flow, transient effects and topography with a more sophisticated 3-D numerical model. Both studies already identified the surface temperature distribution as one of the most sensitive parameters for an accurate temperature prognosis. The interpretation of new subsurface temperature measurements obtained now at the Sedrun site, at the central part of this tunnel, represent an important further step for the recognition of the large-scale Alpine subsurface temperature. The modelling approach presented here covers a nearly complete set of thermally relevant processes active under Alpine conditions by considering additionally effects of uplift and exhumation which are potentially of importance for the subsurface temperature field in

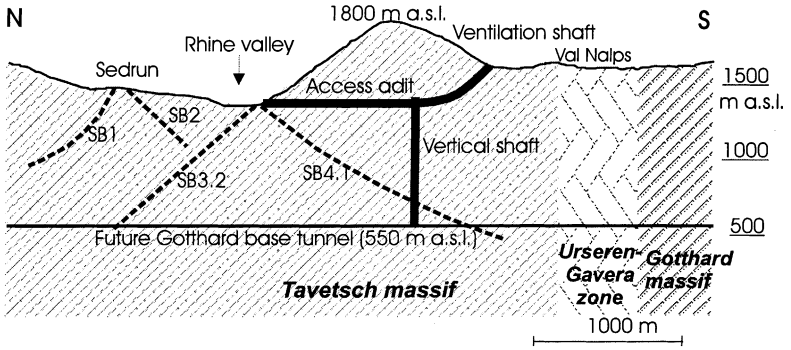

Fig. 1. Construction plan of the intermediate "point-of-attack" at Sedrun with the four exploration boreholes SB1, SB2, SB3.2 and SB4.1. The vertically oriented geological units are indicated by different structure symbols (adapted from AlpTransit Gotthard, 1998).

the central Alps. It will be shown that an accurate evaluation of the subsurface temperature field must not only include a determination of the basal heat flux and rock properties, but also the effects of topography and local ground surface temperature (GST) distribution.

2. Temperature data

2.1. Historical temperature data

In temperature predictions previous observations and corresponding experience in tunnelling must be considered. Especially in the early days of deep Alpine tunnelling this experience (and interpretations) originated from the Swiss Alps. Rock temperature measurements were made already in the "old" Gotthard railway tunnel (1872–1882). The maximum measured temperature was 31°C below a cover of 1700 m. Based on these measurements Königsberger and Thoma (1906) carried out the first analytical temperature calculation for the southern part of the railway tunnel. During the building of the Lötschberg railway tunnel (1906–1913) temperature measurements were taken every 50 m (Gesellschaft für Ingenieurbaukunst, 1996).

The maximum temperature of 34°C occurred below an overburden of 1460 m. During the construction of the Simplon railway tunnel (1898–1906), a maximum temperature of 51°C below an overburden of 2200 m was measured. Because of this high temperature specially efficient cooling and ventilation was needed. Subsequently Niethammer (1910) calculated a 2-D temperature distribution using existing rock and surface temperature measurements. Early attempts to develop temperature prediction methods were based on these observations (Königsberger and Thoma, 1906; Andreae, 1958). Birch (1950) was probably the first to explain measured tunnel temperatures by calculating analytically the 3-D temperature field beneath an arbitrary topography and considering additionally the transient effects of surface uplift.

2.2. Temperature measurements at Sedrun

Temperature has been measured during the construction of the access adit and the shaft. The same method designed and described by Busslinger and Rybach (1999a) has been used to measure the ambient rock temperature: specially drilled, ∼10° down dipping, approximately 6 m long boreholes in the side wall with a diameter of 33 mm were filled with water. After having reached equilibrium the temperature was measured with a calibrated PT100 sensor. This method has proven to be reliable, low-cost and easily practicable by the drilling crew and shall also be applied in future tunnelling programmes of the NEAT project.

With the exception of the first 500 m, temperature data in the access adit has been measured at approximately 50 m intervals 1 week after the advancing tunnel face has passed the measurement site. Repeated additional measurements 1 and 3 months later have indicated generally very little temperature variation. The maximum temperature difference encountered after 3 months was 0.06 K, and the mean standard deviation was 0.03°C for the sidewall holes. The temperature data from the 6 m boreholes is shown in Fig. 2a, together with temperature of water entries which represents the only temperature indicator within the first 500 m. The accuracy of the repeated measurements has already been demonstrated by Busslinger (1998) who showed that the influence of ventilation and cooling devices used for the construction can be ignored if the measurements are taken within 1 week after tunnel drilling machines left the measurement location. Using a simple 1-D analytical solution (Carslaw and Jaeger, 1959) which overestimates the true temperature propagation around a tunnel

$$T = \Delta T \operatorname{erfc}\left(\frac{\Delta x}{2\sqrt{\kappa t}}\right) \quad (1)$$

it can be estimated that a sudden temperature drop at the tunnel wall of $\Delta T = 10$ K has an effect in a medium of a thermal diffusivity, κ, of 10^{-6} m^2 s^{-1} of less than 10^{-2} K over a minimum distance into the wall of $\Delta x = 3.6$ m when measured within $t = 1$ week.

The construction concept applied for the shaft sinking required a slightly modified measurement procedure. The side boreholes could only be drilled when a major break took place during shaft sinking. Thus, at approximately 70 m intervals various measurements have been performed with borehole depths between 3.0 and 4.2 m. The progressing casing of the shaft prevented repeated measurements except at a 3.0 m long side borehole where a standard deviation of 0.3 K was established by three measurements

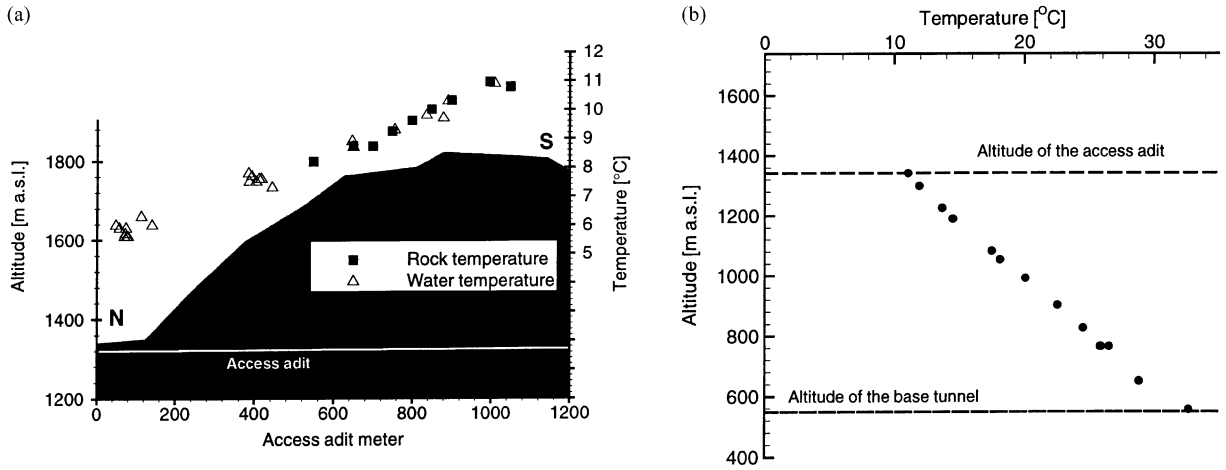

Fig. 2. Temperature data in the access adit (left) and in the shaft (right). The topographic altitude in the profile of the access adit is shown on the left ordinate whereas the right ordinate illustrates measurements of rock temperature and temperature of in-flowing water.

within 1 week. In Fig. 2b, the shaft temperature measurements can be recognised with the repetition data at an altitude of 765 m a.s.l. The different temperatures can be well explained by circulating air since successively measured data decreased with time due to the 5–10 K cooler air temperature in the shaft.

The drilling of the exploration boreholes SB1, SB2, SB3.2 and SB4.1 from the surface (see Fig. 1) was intended especially to assess the hydraulic and rock mechanical properties with temperature logging being only of secondary importance. Especially the data from SB1 and SB2 are of low quality due to too short standing times after drilling or due to fluid flow perturbation. The two logs run in SB3.2 can be identified in Fig. 3a by a temperature offset caused by the different standing times: the first log along the upper part was run immediately after drilling down to ~700 m, the second was run after 5 months standing time and thus

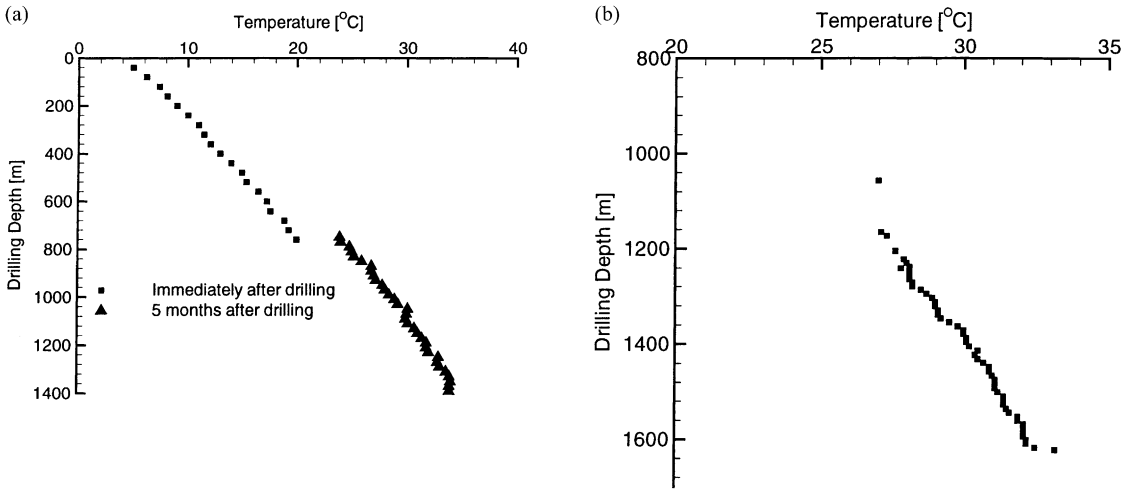

Fig. 3. Temperature logs of (a) SB3.2 and (b) SB4.1. Note, due to the borehole inclination the drilling meters do not represent true vertical depth.

represents the most reliable data. The temperature at depth of the base tunnel in ∼550 m altitude a.s.l. was accessed by the shaft (32.7°C, see Fig. 2b) and by the SB4.1 borehole (32.2°C at ∼1600 m drilling depth, see Fig. 3b). Effects of short standing time at SB4.1 are visible by a temperature offset near bottom hole. Additionally, the strong inclination might have caused a friction-induced non-continuous lowering of the temperature probe which is also visible as "jumps" in the temperature log. The shaft measurement indicates therefore the more reliable data.

It may thus be concluded that out of the four different borehole logs only two of them seem to be interpretable — a fact which highlights the necessity for a rigorous analysis of temperature data collected from boreholes drilled for other purposes than the acquisition of reliable temperature measurements.

Thermal conductivity has been determined on samples originating from the adit and shaft. Measurements taking into account the strong anisotropy were made perpendicular and parallel to the cleavage. The values have been combined with measurements on surface samples along the trace of the future Gotthard base tunnel by Busslinger (1998) who measured 50 samples of the Tavetsch massif and neighbouring lithologies (see later Section 4.1). The parallel and perpendicular components of thermal conductivity for a specific lithology represent the average between 8 and 23 samples ($\sigma \sim \pm 12\%$). Since less heat production values have been determined in the investigation area, additional data were taken from the literature (Rybach and Čermák, 1982).

2.3. Preliminary data evaluation

A conventional Péclet number analysis of the borehole and shaft data represents a customary approach to preliminary heat flow data interpretation. Based on a l-D steady-state diffusive–advective thermal energy equation, a mean vertical fluid flow velocity and a basal heat flow can be estimated (e.g. Jobmann and Clauser, 1994). The heat flow at depth $q(z)$ is calculated with that procedure by

$$q(z) = q(z_1) \exp\left((z - z_1)\frac{Pe}{L}\right) \quad (2)$$

where $q(z_1)$ is heat flow at the lower depth z_1 of a zone with thickness L, and Pe is the dimensionless Péclet number which describes the ratio of convective to conductive heat flow in the case of fluid advection by

$$Pe = v(\rho c)_f \frac{L}{\lambda} \quad (3)$$

with v is the 1-D Darcy velocity ($m\,s^{-1}$), $(\rho c)_f$ the specific heat capacity of fluid, and λ the thermal conductivity of saturated rock. In a plot of the logarithm of $q(z)$ and depth, the slope of $q(z)$ can yield the fluid velocity under ideal 1-D conditions.

By this method a preliminary data evaluation of the vertically oriented profiles like boreholes or shafts was performed; however, the data from the horizontal access adit needed to be evaluated by a multi-dimensional approach. Fig. 4 shows results of the Péclet analysis for the temperatures profiles of the boreholes SB3.2, SB4.1 and the shaft. The heat flow profiles were calculated along the total measured depth range using a thermal conductivity of $3.61\,W\,m^{-1}\,K^{-1}$ (mean of the measured vertical component in Tavetsch massif) and temperature gradient values for a given interval length in the boreholes and from neighbouring temperature data in the shaft. Strong heat flow fluctuations at the boreholes could be suppressed by increasing the interval length up to ∼20 m; further increase of the interval length did not strongly change the main characteristics. Care was taken to correct the data from the inclined borehole for a vertical profile. The regression lines calculated from $\ln(q(z))$ — profiles yield similar values for bottom hole heat flow but different values for flow velocities (Fig. 4). Bottom hole heat flow at boreholes SB3.2 (Fig. 4a) and SB4.1 (Fig. 4b) is indicated by 101 and $108\,mW\,m^{-2}$ at altitudes of 545 and 579 m a.s.l. (corresponding to 760 and 800 m depth) whereas a value of $99\,mW\,m^{-2}$ at 830 m a.s.l. is given at the shaft (Fig. 4c). Fluid flow at SB3.2 and shaft is upwards directed with magnitudes of 23 and 7 mm per year, respectively, whereas at SB4.1 flow is downwards directed with a 20 mm per year magnitude. The large vertical variation of heat flow derived from the regression line suggests that the coincidence of the heat flow values at the bottom hole happened accidentally. In spite of the low quality of the borehole data, this Péclet analysis highlights the main problem encountered in Alpine terrain: the generally used approaches to explain temperature data by 1-D steady-state

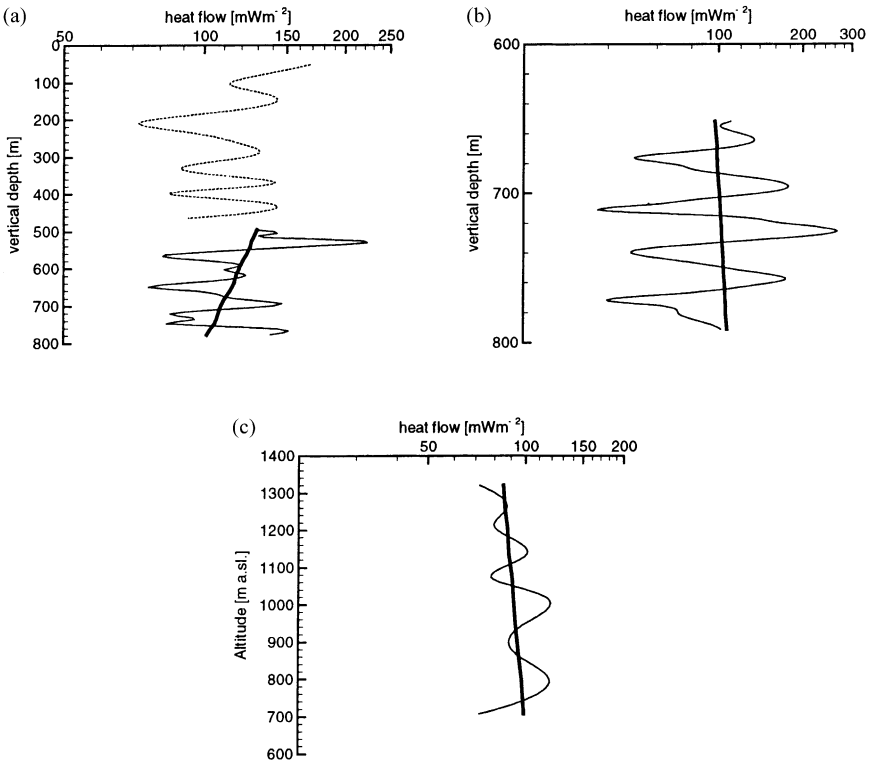

Fig. 4. Péclet number analysis for the (a) SB3.2; (b) SB4.1 boreholes; and (c) the shaft. The depth scale is true vertical depth. With the exception of the first temperature log in SB3.2 all variable $q(z)$ profiles have been fitted by a regression line.

assumptions do not hold! Along the investigated depth range neither the heat flow nor the fluid velocities indicate identical values in an area which extends laterally only over 2 km. Nevertheless, these observations provide a hint to the complexity of the temperature data taken from high Alpine terrain and emphasises the need for a much more careful analysis which accounts for various physical effects that may influence subsurface temperature.

3. Thermal conditions in Alpine subsurface

It is intended in the present model approach to include not only all structural effects such as topography and lithology, but also various physical processes that are potentially of influence on the Alpine subsurface temperature fields. In this section, the procedure used to evaluate the 3-D thermal conditions at the Sedrun location is described. In a region of high relief the usually observed temperature increase with overburden can be influenced by 3-D topography, geological zones with different thermal conductivity, water circulation, erosion and uplift. In addition, transient effects such as glacially-induced cold periods may occur. Former experience in simulating Alpine subsurface temperature field (Busslinger and Rybach, 1999b) has elucidated the significance of an exact representation of 3-D topography and geology, but also of various thermally relevant processes such as transient climatic effects and fluid flow. Here, we intend to describe thermal transport by a comprehensive analysis which also considers effect of surface temperature distribution and of uplift/erosion. In the next subsections, the individual assumptions taken in our modelling approach will be described in more detail. The transport of heat in the subsurface is calculated assuming the following equation based on thermal energy

conservation

$$\underset{\text{transient}}{\langle \rho c_p \rangle \frac{\partial T}{\partial t}} = \underset{\text{diffusion}}{\nabla(\langle \Lambda \rangle \nabla T)} - \underset{\text{fluid advection}}{[\rho c_p]_f v \nabla T} - \underset{\text{mass advection}}{\langle \rho c_p \rangle V \nabla T} - \underset{\text{source}}{Q} \quad (4)$$

with $\langle \rho c_p \rangle$ as the thermal capacity of the saturated rock, T the temperature, t the time, $\langle \Lambda \rangle$ the thermal conductivity tensor of the saturated rock, $[\rho c_p]_f$ the thermal capacity of the fluid, v the Darcy fluid velocity, V the mass advection velocity and Q the heat sources.

3.1. Transient model

At least in the last 10^6 years but probably during the whole Alpine evolution (200 million years) the climatic history of the Alps underwent large changes. The GST variation which most perturbed the subsurface temperature field in central Europe (e.g. Kohl, 1998a,b) was during the last Pleistocene Ice Age. Assuming a 10°C cooler surface temperature during the period 70,000–10,000 years b.p. (e.g. roughly the duration of the last glacial) and a typical thermal diffusivity of $10^{-6}\,m^2\,s^{-1}$, the cooling effect extends down to depths of 2000 m. Such an event still causes at the surface a heat flow difference of $-18\,mW\,m^{-2}$, or at a depth of 1000 m a temperature difference of more than −4 K compared to steady-state conditions. More recent climatic events such as temperature variations during the last centuries or the recent warming period cause much smaller temperature changes and did not yet penetrate to greater depth. In the modelling approach, we assume the reference GST history for central Europe used by Kohl (1998a,b) starting at $t = 10^5$ years b.p., but with a 10 K instead of 8 K cooler surface temperature during the last Ice Age. This assumption is based on the argument that periglacial climatic conditions during the latest glaciation epoch can create a relatively cool environment (see also Kukkonen et al., 1997). The assumed GST history also accounts for more recent, lower amplitude temperature variations such as the 1 K warming during this century. At the depth of our investigation which extends down to 1600 m below surface, the last Pleistocene Ice Age has the largest impact on the temperature field.

A different effect is caused by the uplift history of the Swiss Alps. Different geological model assumptions explain the movement of this mountain belt during its whole evolution (Burkhard, 1999). Since the reconstruction of uplift history in the Swiss Alps currently based on 1-D interpretation of fission-track data (Michalski and Soom, 1990) does not show consistent results, sensitivity calculations were performed to evaluate the effect of a variable transient uplift rate (see below). They indicated that an uplift history starting 5 million years b.p. is sufficiently far to define starting conditions for mass advection. Thus, the following transient events were considered: a constant rate uplift history of mass advection starting 5×10^6 years b.p., the surface temperature variation starting 10^5 years b.p., and water circulation starting at the end of the last Ice Age (10^4 years b.p.).

3.2. Fluid and mass advection

Fluid flow is calculated from Darcy's law assuming a linear relationship between hydraulic head gradient and flow velocity. Rock permeability variations over two orders of magnitude from 10^{-17} to $10^{-15}\,m^2$ easily occurring in the active tectonic regime of the central Swiss Alps (e.g. Busslinger and Rybach, 1999b) may switch the thermal field from diffusive to advective dominated (see Smith and Chapman, 1983). It thus, can be assumed that fluid flow in crystalline rock easily will play either a strongly dominating or a completely insignificant role. Therefore, the hydraulic flow field needed to be considered and appropriate steady-state boundary conditions were set (i.e. the hydraulic head was set as first order approximation to topographic surface) but hydraulic parameters were initially taken so low that fluid flow does not influence the heat transport field.

From actual geodetically determined uplift rates in the Swiss Alps (Geiger, personal communications, ETHZ, see also Schlatter and Marti, 1999) the magnitude of mass advection could be established. In the area around Sedrun uplift seems to vary linearly between 0.9 and 0.65 mm per year on a SE–NW striking profile at distances of 25 km from Sedrun. For the Sedrun location magnitudes of 0.75 mm per year can be approximated which are ∼20% higher than the past exhumation rates determined from Apatite fission-track data (Michalski and Soom, 1990). In agreement with a tectonic model established by Pfiffner and Heitzmann (1997) the lateral component

Table 1
Difference between mean air and mean ground surface temperature (Bendel, 1948)

Altitude (m a.s.l.)	0	500	1000	1500	2000	2500
Temperature difference (ground–air (°C))	0.8	1.0	1.3	1.7	2.3	3.0

in mass advection was neglected. Pfiffner and Heitzmann (1997) predict a nearly vertical uplift in this part of the Swiss Alps due to an active thrust of the Gotthard and Aar massif with a ramp at ∼10 km depth (see also Burkhard, 1999). It was assumed in the model approach that uplift equals exhumation rate, i.e. the shape and position of topography does not change with time.

To our knowledge it never has been shown that the critical uplift rate which perturbs a steady-state diffusive temperature field depends strongly on the postulated uplift length. This can be easily shown in terms of the Péclet nmber, *Pe*, defining now the ratio between thermal transport driven by mass advection and by diffusion

$$Pe = \frac{q_{\text{adv}}}{q_{\text{diff}}} = \frac{\langle \rho c_p \rangle V_z L}{\lambda_{zz}} \tag{5}$$

with V_z the uplift/exhumation rate, λ_{zz} the vertical component of the thermal conductivity tensor and L the characteristic uplift length of the system.

A general characterisation can be performed for systems with $Pe > 1$ illustrating advective and $Pe < 1$ illustrating diffusive dominated temperature fields. From $Pe > 0.1$ the advection effect on the thermal field starts to manifest and needs to be accounted for. Thus, uplift along a short depth range must be much faster to create a thermal signature than uplift along deep crustal scale. Supposing a thermal diffusivity, κ, of $10^{-6}\,\text{m}^2\,\text{s}^{-1}$ ($\kappa = \langle \rho c_p \rangle / \langle \Lambda \rangle$) $Pe > 0.1$ is fulfilled for $L = 12\,\text{km}$ and $V_z > 0.25\,\text{mm}$ per year or $L = 6\,\text{km}$ and $V_z > 0.5\,\text{mm}$ per year. It may be noted that similar considerations are applicable and are implicitly used for evaluating the impact of fluid flow to a thermal field.

3.3. Surface temperature data

It is customary to take the mean annual air temperature as a substitute for the GST. However, a systematic bias is introduced by doing so. Extensive investigations show that the annual average GST, in areas which have snow cover in winter, is always higher than the mean air temperature. This is mainly due to thermal insulation of the snow layer covering the earth's surface: during cold days (with temperatures far below −10°C) the ground hardly cools below 0°C, with well-known agricultural benefits. The difference between mean air and ground temperature increases with altitude in central Europe, as shown in Table 1.

In the first temperature prediction for the Gotthard base tunnel done by Rybach and Pfister (1994) sensitivity runs have shown that the surface temperature is of great importance for the prediction of the rock temperature. Since only a very small set of GST data for the Gotthard area exist, the usual linear and dependence on altitude model necessarily has to be taken, which is also based on data of the Swiss Meteorological Institute (SMA).

$$T_s = T_0 - \alpha z \tag{6}$$

with T_s the GST at topographic surface, T_0 the GST at sea level, α the atmospheric lapse rate and z the altitude (see also Fig. 8).

A severe restriction of this model needs to be emphasised: GST not only depends on altitude but furthermore on the exposition to radiation of the local surface which can be quantified from slope angle and orientation (e.g. Blackwell et al., 1980), on the vegetation (e.g. Lewis and Wang, 1992) and on the rock surface structure. Previous approaches to quantify these effects have been done assuming a homogeneous soil cover which does not change its character. Due to the complex situation in the Alpine environment, there are no investigations which tried to quantify the GST on steep, high topographies with soil cover varying between exposed rock and vegetation/forest. A rough idea of this effect under these conditions can be extracted from GST determinations

of Niethammer (1910) measured in the framework of the Simplon railway tunnel construction. Recently, Wegmann et al. (1998) have measured GST differences of nearly 10°C in the surroundings of two specific locations in the Swiss Alps. There are however, more datasets available at lower topographies with more homogeneous vegetation cover indicating smaller GST variations at the same altitude (e.g. Defila and Brändli, 1989 or Šafanda, 1999). Since no comprehensive analyses have been performed until now for the Swiss Alps we thus have to assume local conditions at each specific site (see below).

3.4. Numerical FE procedure

The problem related to simulating subsurface temperature effects due to topographic perturbation has been studied since the beginning of the century (see Kohl, 1999 for details). The challenge to simulate temperature fields below Alpine settings requires the representation of physical and structural settings as closely as possible in a numerical treatment since each of them may cause thermal impacts and therewith influences the final interpretation. The assignment of structural data such as geology and topography in a discretisation scheme is accomplished by the mesh generator WinFra (internal report Kohl, 1998b) supplying a graphical user interface with CAD capabilities whereas the numerical simulations which account for various physical processes are performed by the finite element (FE) code FRACTure (Kohl and Hopkirk, 1995).

During mesh generation special emphasis is given to the representation of topography which is calculated from a digital terrain model (DTM). In our approach a 250 m × 250 m DTM of Switzerland has been used. In a CAD type approach firstly a 2-D model will be defined which originally represents an arbitrary horizontal section of the final 3-D model. Since the procedure intends lateral boundaries be finally characterised by thermal and hydraulic "no-flow" boundary conditions the lateral boundaries of the initial 2-D section are set mostly on topographical arguments. Only valleys and ridges represent possible topographic structures with lateral hydraulic and thermal no-flow conditions. Since heterogeneities may have a strong influence on the subsurface flow field it is best they be placed at large distances from the area of investigation (details below). Experience from hydraulic data acquisition in the south Gotthard region (AlpTransit Gotthard, 1993) has demonstrated that the subsurface hydraulic flow field may extend over large distances and can be only accounted for if the area of investigation is placed in a sufficiently large model. The 3-D mesh is then continuously developed in further steps by defining a first flat 3-D geometry, by stretching individual layers of this geometry along the interpolated DTM data, by attributing various lithologies to this model and finally by local or global refinement.

4. Modelling

4.1. 3-D model geometry and geological units

The area of investigation around the shaft is situated in a mountain rising 400 m above the valley bottom south of Sedrun (see Fig. 1). In a 6 km radius around Sedrun much higher mountains of the central Swiss Alps up to 3000 m a.s.l. (i.e. 1500 m above the altitude of the valley) can be encountered. Clearly, when evaluating the subsurface temperature field this situation requires one to account for the topography as a source for possible thermal perturbation. There are no 2-D structures like parallel ridges which would allow a simplification to the modelling approach.

As already mentioned the imposed boundary conditions at the lateral boundaries require a sufficiently large model extension with boundaries placed at distances between 10 and 15 km from the shaft. Near the shaft, the model was refined down to element sizes of <80 m; towards the boundaries, element sizes of up to 600 m were chosen. The lower boundary of the model was placed at −10 km a.s.l., producing a total vertical model range between 11 and 13 km. Various 2-D sensitivity model runs indicated this range was sufficiently large for the basal heat flow boundary conditions taken in our model (Signorelli, 1999). They were also used to determine the degree of vertical refinement: 2500 m intervals below −2500 m, 500 m intervals between −2500 and 500 m and finally intervals <100 m near the surface, depending on the topography (see Fig. 5) were used. The total mesh consisted of nearly 50,000 nodes.

The geological model is based on the interpretation of seismic profiles through the central Swiss

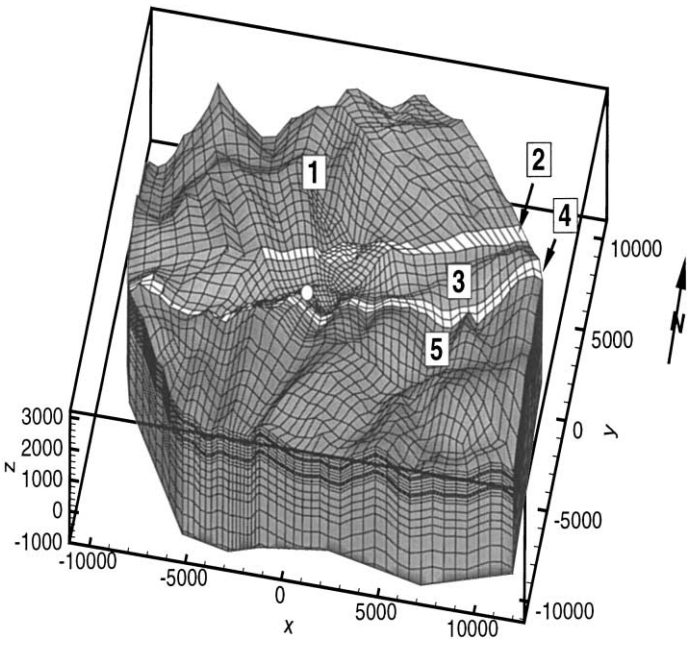

Fig. 5. Overview of the 3-D FE discretisation of the region Sedrun. The figure illustrates the uppermost layers ($z > -1000$ m) to enhance the overview. The vertical axis is scaled by a factor 2. The location of the shaft is situated on $x/y = 0/0$ and is marked by a white circle. The adit and the boreholes are situated on a N–S oriented profile acrossing the shaft. The numbers identify the geological units. 1: Aar massif; 2: Clavaniev zone; 3: Tavetsch massif; 4: Useren–Carvera zone; and 5: Gotthard massif. The total model encompasses 50,000 nodes.

Alps (Pfiffner and Heitzmann, 1997). The discretised model includes five geological units: Aar massif, Clavaniev zone, Tavetsch massif, Useren–Carvera zone and Gotthard massif (see Fig. 5). The high dip angles of the three zones Tavetsch massif, Clavaniev zone and Useren–Carvera zone which are sandwiched between the main crystalline Gotthard and Aar massifs, were represented by vertically oriented geological units down to −5000 m a.s.l. The same uplift rate of 0.75 mm per year is attributed to all five lithologies. The lowermost layer represents the zone in which the deep SE–NE oriented lateral mass transport supplied from excess mass of the European–African collision turns near vertically. The geological units are characterised by different thermal (thermal capacity and conductivity, heat production) and hydraulic (hydraulic conductivity) properties (see Table 2). Due to the strong anisotropy all tensor components of thermal conductivity needed to be considered calculated from the orientation of cleavage (AlpTransit Gotthard, 1995).

Table 2
Thermal properties of the different geological units

Geological unit	Aar massif	Clavaniev zone	Tavetsch massif	Urseren–Garvera zone	Gotthard massif
$\langle\Lambda\rangle$ parallel to cleavage ($W\,m^{-1}\,K^{-1}$)	3.66	4.04	3.61	3.10	4.43
$\langle\Lambda\rangle$ perpendicular to cleavage ($W\,m^{-1}\,K^{-1}$)	2.83	3.04	2.79	2.45	2.95
Dip of cleavage	89°S	89°S	90°	90°	60°N
$\langle\rho c_p\rangle$ ($J\,m^{-3}\,K^{-1}$)	2.6×10^6	2.6×10^6	2.6×10^6	2.6×10^6	2.6×10^6
Heat production ($\mu W\,m^{-3}$)	2.4	2.5	2	2.6	2.1

5. Results and discussion

5.1. Model fit

In the forward modelling procedure to investigate the temperature datasets measured at the Sedrun point-of-attack, the lithological units and thermal parameters were not changed. Rather, the measured subsurface temperature data were fit by varying the values of hydraulic conductivity, GST distribution and basal heat flow. Clearly, the model results depend upon the validity of the assumed thermal mechanisms described in Section 3 and the validity of near-surface parameters values for greater depth. By this procedure it is intended to demonstrate the feasibility of thermal analyses in complex settings rather than providing or quantifying the well-known non-uniqueness in the solution of diffusive processes. In that manner, the basal heat flow value determined as $74\,\mathrm{mW\,m^{-2}}$ at -10 km a.s.l. represents such a model parameter which may vary depending on the validity of individual transport mechanisms. For example, a lower basal heat flow value would result from a temperature dependency of thermal conductivity with 10% lower values at 100°C or from deeper roots of the uplifted massifs (cf. Section 3.2).

The topographic effect at the shaft location is manifested clearly by the variation in the vertical heat flow component, $q(z)$. Its magnitude is proportional to the basal heat flow value for a pure diffusive steady-state model without radiogenic heat production (i.e. ignoring any transient effect or advection). At the shaft location this effect causes a $q(z)$ variation from surface ($\Delta q = -19\,\mathrm{mW\,m^{-2}}$) to the altitude of the access adit ($\Delta q = -12\,\mathrm{mW\,m^{-2}}$) down to the depth of the future base tunnel at 550 m a.s.l. ($\Delta q = -4\,\mathrm{mW\,m^{-2}}$). Note, that an increasing q with depth is also visible in Fig. 4c. In the final model with all mechanisms activated, $q(z)$ decreases again at greater depth mainly due to the effect of radiogenic heat production. The superposition of heat production, climatic and uplift effect on the topographic effect yields a very complex interplay of thermally relevant mechanisms which can no more be treated analytically. The surface heat flow pattern illustrates these statements: in the Rhine valley, a maximum surface heat flow of $>100\,\mathrm{mW\,m^{-2}}$ is contrasted by a surface heat flow of $<40\,\mathrm{mW\,m^{-2}}$ at the mountain locations. It may be noted that the horizontal heat flow component, usually neglected in the subsurface, reaches values $>30\,\mathrm{mW\,m^{-2}}$ at surface (mid flanks) with maximum components oriented perpendicular to the valley orientation.

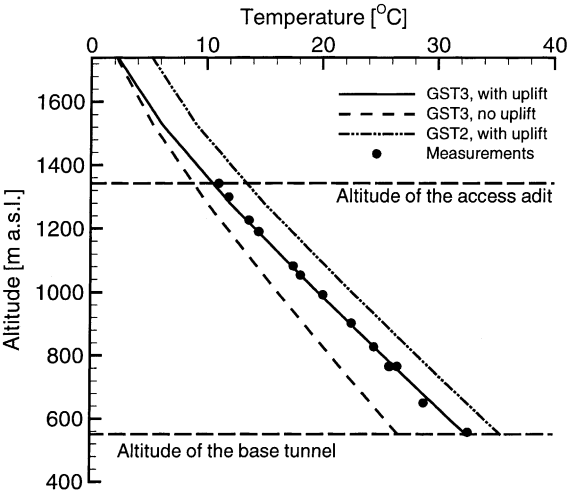

Fig. 6. Temperature distribution along the shaft for model GST2 with uplift GST3 without uplift and GST3 with uplift (best fit model). Note, the best fit model also matches the corresponding temperature data of the SB4.1 borehole at ~750 m which crosses the shaft at ~40 m lateral distance. See text for further explanations.

All reliable thermal data can be nearly perfectly fitted by the best fitting model. Fig. 6, for the 800 m deep shaft, and Fig. 7a, for the 1200 m long access adit, illustrate a maximum ± 1 K deviation in temperature of the best model fit from measurements. The most reliable data of the borehole temperature logs such as the second log in SB3.2 or BHT values of both boreholes were also well matched by this model (Fig. 7a and b). The only consistent deviation from reliable temperature data can be found along the adit between 500 and 700 m. The predicted temperatures are here ~1 K above the measured data, an effect that could be attributed to downward percolating fluid movement in near-surface layers. The curvature in the temperature profile at ~1500 m altitude a.s.l. (i.e. 80 m above the shaft head) is due to the assumed $+1$ K warming in this century, whereas, effects of Pleistocene Ice Age manifests mostly below the altitude of the base tunnel.

Generally, the best fit models are nearly insensitive to any hydraulic impact. Hydraulic conductivity values of $K = 10^{-10}\,\mathrm{m\,s^{-1}}$ in the Aar and Gotthard

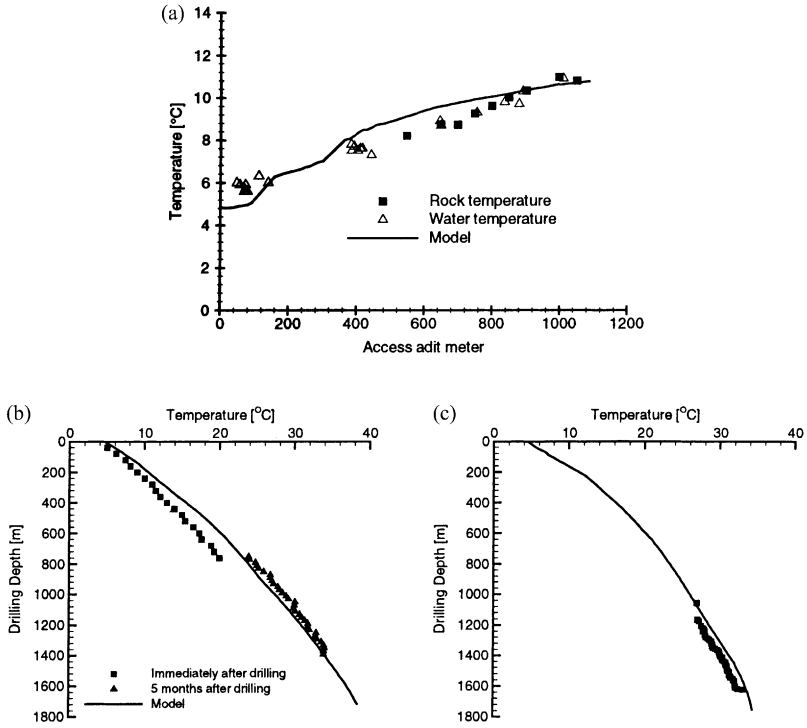

Fig. 7. Comparison measurement and model prediction for the access (a) adit, boreholes; (b) SB3.2; and (c) SB4.1. Prediction of model GST3 is indicated by a continuous line.

massifs and $10^{-9}\,\mathrm{m\,s^{-1}}$ (data adapted from Wyder and Rybach, 1996) in the tectonically strongly deformed Tavetsch massif, Clavaniev zone and Useren–Carvera zone have been assumed in this best fit model run. These hydraulic conditions result in low Péclet numbers between 0.01 and 0.15 at surface. For the assumed hydraulic boundary conditions these hydraulic conductivity values represent nearly maximum estimations: an increase by one order of magnitude would yield a significant advective transport ($Pe > 1$) not supported by the data. It may be noted that this procedure has largely overestimated the hydraulic gradient because the real water table in Alpine terrain has usually a much flatter gradient (e.g. measurements performed by AlpTransit Gotthard (1993) or model investigations by Forster and Smith (1988). For a 90% smaller gradient the same maximum fluid flow field could be reproduced by 10 times higher hydraulic conductivity value (i.e. maximum $K = 10^{-8}\,\mathrm{m\,s^{-1}}$). The magnitude of the flow velocity at the shaft postulated from the Péclet analysis discussed above is strongly exaggerated mainly due to the neglected topographic effect. Our model indicates here maximum flow velocities of only 0.8 mm per year.

Before and during this investigation further detailed 2-D and 3-D sensitivity studies illustrated in Fig. 6 have been performed at the shaft location (Signorelli, 1999). They represent the result of more detailed investigations and will be described in the following sections.

5.2. Surface temperature effect

Lack of GST measurements in Alpine settings their importance for the Alpine subsurface temperature distribution can only be approached by model assumptions reasoned by sensitivity studies. The specific site of Sedrun is dominated by the northern, shady slope of the mountains (see also Fig. 5). Since the determination of the local GST variation offers infinite possibilities it was intended to leave the value of the atmospheric lapse rate unchanged but rather to

change the value for surface temperature at sea level T_0 (cf. Eq. (6)). It is thought that the GST variation is determined by local, not altitude-dependent conditions such as radiation, vegetation, snow cover or surface structure, and by the regional atmospheric lapse rate. Clearly, this approach integrates over small-scale effects due to varying topographic orientation or wind conditions. In that manner, three different surface temperature models have been investigated with a nearly identical atmospheric lapse rates α but a variable T_0 offset.

- Model GST1 with $T_0 = 11.88$ and $\alpha = 0.0046$ K m^{-1} which was employed by Niethammer (1910), based on own measurements. Such regression line fits his data within ± 2.35 K.
- Model GST2 with $T_0 = 13.50$ and $\alpha = 0.0048$ K m^{-1} which is based on SMA data and was assumed in several modelling approaches in the Swiss Alps (e.g. Busslinger and Rybach, 1999b).
- Model GST3 with $T_0 = 10.20$ and $\alpha = 0.0048$ K m^{-1}, which represents the result of a best fit model for the Sedrun location. The low T_0 value is considered to be due to the local north-slope.

The different GST models together with available data from the Alpine region are illustrated in Fig. 8. The GST2 assumption seems to fit best the temperature at lower altitudes, whereas the large scattering of surface data collected from higher altitudes tends to be better fitted by GST1. Model GST3 clearly is on the lower bound of these data.

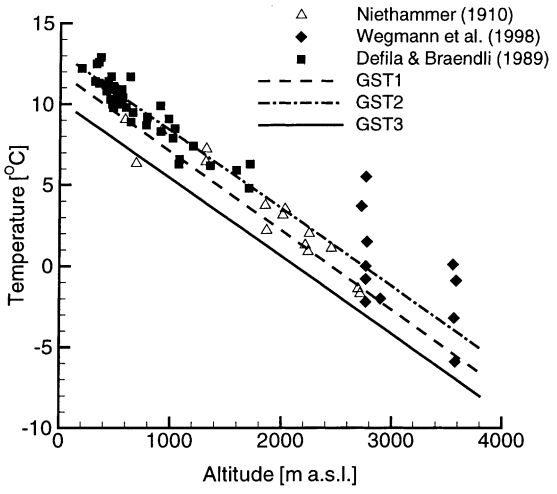

Fig. 8. Surface temperature models and available data from Alpine terrain. For definitions of GST1–GST3 see text.

The sensitivity runs indicate that even for a complex interplay of transient and steady-state thermal mechanisms the assumption of different GST models result in a nearly uniform temperature offset in subsurface. This becomes evident in Fig. 6 indicating the difference between GST2 and GST3.

5.3. Uplift effect

Earlier numerical temperature simulations from Alpine terrain (e.g. Rybach and Pfister, 1994 or Busslinger and Rybach, 1999b) do not explicitly account for uplift and exhumation. When fitting measured temperature data such approaches implicitly accommodate the mass advection effect by a more or less pronounced increased basal heat flow value depending on the magnitude of advection. In this section the effect of uplift and exhumation will be described for the 3-D model used for the Sedrun location. As mentioned earlier our model approach assumes surface elevation change to be zero (i.e. uplift rate equals exhumation rate, see also England and Molnar, 1990).

For evaluating the sensitivity of mass advection to the subsurface temperature field (see also Section 3.2) the uplift effect in our 3-D model was quantified for the example at the shaft location. For the purpose of a sensitivity analysis, the difference between the pure diffusive and combined diffusive–advective GST3 model is illustrated in Fig. 6. When linearising the temperature effect of mass advection — which is valid for the uplift range between 0.5 and 1 mm per year — the importance of mass advection is demonstrated by the fact that a variation of uplift by 0.1 mm per year yields already a temperature variation of 0.4 K at the level of the future base tunnel in 550 m altitude a.s.l. (Signorelli, 1999). Clearly, at larger uplift rates, this effect becomes more prominent. The uplift rate of 0.75 mm per year taken in this simulation causes an additional heat flux of more than 10 mW m^{-2} at surface. Evidently, it is this value that need to be subtracted from the basal heat flow of a pure diffusive model of a non-moving medium to compensate for the mass advection effect.

Further sensitivity analyses considered the moment at which transient changes of uplift become invisi-

ble in the present temperature field. Geochronometric investigations based on determination of Apatite and Zircon fission-track ages reveal an increase of uplift during the last 20×10^6 years (e.g. Michalski and Soom, 1990). In our analysis we assumed a stepwise increase of uplift from 0.3 (20×10^6 years ago) to 0.75 mm per year (present day value) with intervals lasting approximately 4×10^6 years. This investigation displayed two results: firstly, at the given interval length the present day temperature field is insensitive to any preceding changes in uplift rate and secondly, 5×10^6 years of uplift history is a sufficient long time interval to approach steady-state conditions even at surface.

6. Conclusions

Several temperature datasets collected in the central Swiss Alps near Sedrun — a terrain which is dominated by steep and highly variable topography and crystalline rock outcropping at surface — at depth ranges extending down to 1200 m depth could be well explained by the present model approach. For this purpose, a 3-D numerical model had to be developed accounting for topographic and structural effects as well as for various thermally relevant mechanisms such as mass advection or transient signatures. The high quality rock temperature measurements performed in the 800 m deep shaft and the data of the 1200 m long access adit with high overburden could be accurately fitted (maximum deviations ± 1 K). Furthermore the main characteristics and most reliable data (BHT values of the low quality temperature logs from strongly inclined, >1.5 km long boreholes) were also well matched. A very interesting fact of this model approach should be emphasised: our model basically uses only elementary and evident data and assumptions such as topography, geological units, uplift rate or palaeoclimatic influence. With the exception of the two principal thermal boundary conditions (local GST model and basal heat flow) no other parameter needed to be adjusted for the model fit. This successful data analysis as well as the results of Busslinger and Rybach (1999a) demonstrate that a temperature prognosis for deep underground constructions is feasible if it is based on a well calibrated model, even under complex conditions.

This procedure has shown the importance of the assumed GST model for the temperature simulations. It points to the fact that it is necessary to take into account the dependence of the surface temperature on slope angle and orientation. In the case of Sedrun, the setting is dominated by the northern, shady slope of a nearby mountain which even causes a thermal impact at depths of >1000 m. The missing surface temperature data indicate the need for more detailed investigations. Future efforts should include not only investigating the extent of the permafrost zone but also measuring local GST variations. With the exception of the kind of investigations such as presented here, there is actually only little information about the mean annual GST as function of altitude, vegetation, settlements, wind condition or surface structure.

The large-scale deep subsurface temperature field at Sedrun does not seem to be influenced by fluid flow at greater depth. The only advective influence manifests at parts of the adit with shallow Quaternary cover and at the two shallowest boreholes SB1 and SB2. Based on these thermal observables the large-scale hydraulic conductivity can be assumed to be $<10^{-8}\,\mathrm{m\,s^{-1}}$, a fact which has a positive impact for the ongoing and planned underground constructions. Such result agrees with data analyses of Busslinger and Rybach (1999a) or Maréchal et al. (1999) who observe temperature in Alpine subsurface to be dominated by diffusive thermal transport. High permeable structures seem to have a prominent large-scale impact on the thermal field only at very exceptional parts such as the large and deep Piora zone in the south of the Gotthard massif (Busslinger and Rybach, 1999a). Both, the observations made at Gotthard and at Sedrun do not support a large-scale hydraulic background influence — either it is restricted to small-scale fault structures or it is visible as a dominant large-scale thermal anomaly. These conclusions, based on a full 3-D model approach, are therewith in contradiction to results from lower-dimensional models claiming the existence of an intermediate hydraulic background influence such as the 2-D interpretation of temperature profiles from the eastern Swiss Alps (Bodri and Rybach, 1998) or the presented 1-D Péclet analysis. As demonstrated here, such lower-dimensional approaches tend to characterise topographic-induced heat flow variations as hydraulic impact instead of purely diffusive driven effect. It may be noted that equivalent misinterpretation

can also occur in case of thermal refraction as demonstrated by Kohl and Rybach (1996).

Furthermore, our model approach also allows to estimate the basal heat flow under high topographies. The results provide the necessary information required to constrain boundary conditions of actual geodynamic model approaches of the Alpine mountain belt. This local model suggests that the Alpine heat flow does not differ strongly from the heat flow in the Swiss lowland (Medici and Rybach, 1995). Due to the strong anisotropy of the geological units and the orientation of individual layers the heat flow field at the Sedrun site is not reflected by elevated temperature values. The correct treatment of structural data such as topography and anisotropy as well as of geodynamic effects like mass advection is therefore indispensable for the successful interpretation of temperature data in Alpine settings.

Acknowledgements

The authors want to thank A. Busslinger for discussions and for supplying of his measurement data for the present analysis. The support of this project by the AlpTransit project management is gratefully acknowledged. Especially appreciated is the cooperation with St. Flury from the AlpTransit project management and with P. Guntli, F. Walker, U. Zehnder for taking responsibility in temperature measurement. The comments of J. Šafanda and of T. Lewis are also gratefully acknowledged. Especially, T. Lewis' suggestions helped to improve the text.

References

AlpTransit Gotthard, 1993. Arbeitsteam Hydrogeologie: Hydrogeologische Modellierung Vorprojekt. 1. Konzeptuelles Modell und Referenzdatensatz, Report No. 1763/7. AlpTransit Gotthard-Basistunnel.

AlpTransit Gotthard, 1995. Gotthard-basistunnel, spezialbericht geologie, geotechnik und hydrogeologie. In: Schneider, T.R. (Ed.), Geologisch-Geotechnisches Längsprofil. Auflageprojekt, Report No. 425 bg/2.

AlpTransit Gotthard, 1998. Info Gotthard: Der neue Basistunnel durch den Gotthard. Public Report.

Andreae, C., 1958. La prévision des températures souterraines, Ann. Ponts et Chaussées, pp. 38–85.

Bendel L., 1948. Ingenieurgeologie. Springer, Berlin.

Blackwell, D.D., Steele, J.L., Brott, Ch.A., 1980. The terrain effect on terrestrial heat flow. JGR B85 (9), 4757–4772.

Birch, F., 1950. Flow of heat in the front range. Colorado Bull. Geol. Soc. Am. 61, 567–630.

Bodri, B., Rybach, L., 1998. Influence of topographically driven convection of heat flow in the Swiss Alps. Tectonophysics 291 (1–4), 19–29.

Burkhard, M., 1999. Strukturgeologie und Tektonik im Bereich Alptransit. In: Löw, S., Wyss, R. (Eds.), Vorerkundung und Prognose der Basistunnel am Gotthard und am Lötschberg. A.A. Balkema, Rotterdam, pp. 45–56.

Busslinger, A., 1998. Geothermische Prognosen für tiefliegende Tunnel PhD thesis ETH No. 12715.

Busslinger, A., Rybach, L., 1999a. Geothermal prediction of water-bearing zones. Tunnel 1, 33–41.

Busslinger, A., Rybach, L., 1999b. Predicting rock temperature for deep tunnel. Tunnel 1, 24–32.

Carslaw, H.S., Jaeger, J.C., 1959. Conduction of Heat in Solids, 2nd Edition. Oxford University Press, Oxford.

Defila, C., Brändli, J., 1989. Bodentemperaturen und Verdunstung, 1951–1985. Klimatologie der Schweiz Heft 28 P. Beiheft zu den Annalen der Schweizerischen Meteorologischen Anstalt. Jahrgang, 1986.

England, P.-C., Molnar, P., 1990. Surface uplift, uplift of rocks, and exhumation of rocks. Geology 18 (12), 1173–1177.

Forster, C.B., Smith, L., 1988. Groundwater flow in mountainous terrain. 2. Controlling factors. Water Resour. Res. 24 (7), 1011–1023.

Gesellschaft für Ingenieurbaukunst, 1996. Historische Alpendurchstiche in der Schweiz, Gotthard, Simplon, Lötschberg. Report at Institut für Bauplanung und Baubetrieb ETH Zürich. Institut für Geotechnik ETH Zürich. Rothpletz, Lienhard + Cie AG.

Jobmann, M., Clauser, C., 1994. Heat advection versus conduction at the KTB: possible reasons for vertical variations in heat-flow density. Geophys. J. Int. 119 (1), 44–68.

Königsberger, J., Thoma, E., 1906. Über die Beeinflussung der geothermischen Tiefenstufe durch Berge und Täler, Schichtstellung, durch fliessendes Wasser und durch Wärme erzeugende Einlagerungen. Eclogae Geol. Helv. 9, 113–144.

Kohl, T., 1998a. Palaeoclimatic temperature signals — can they be washed out? Tectonophysics 291 (1–4), 225–234.

Kohl, T., 1998b. FRACTure (V.3.1), Finite Element Program with WinFra (V.0.56), Internal Report. Institute of Geophysics, ETH Zürich, Switzerland.

Kohl, T., 1999. Transient thermal effects at complex topographies. Tectonophysics 306, 311–324.

Kohl, T., Hopkirk, R.J., 1995. FRACTure: a simulation code for forced fluid and transport in fractured porous rock. Geothermics 24 (3), 345–359.

Kohl, T., Rybach, L., 1996. Thermal and hydraulic aspects of the KTB drill site. Geophys. J. Int. 124, 756–772.

Kukkonen, T.T., Golovanova, I.V., Khachay, Yu.V., Druzhinin, V.S., Kosarev, A.M., Schapov, V.A., 1997. Low geothermal heat flow of the Urals fold belt — implication of low heat production, fluid circulation or palaeoclimate? Tectonophysics 276 (1–4), 63–85.

Lewis, T.J., Wang, K., 1992. Influence of terrain on bedrock temperatures. Glob & Planet. Change 6 (2), 87–101.

Maréchal, J.-C., Perrochet, P., Tacher, L., 1999. Long-term simulation of thermal and hydraulic characteristics in a mountain massif. The Mont-Blanc (Alps) case study. Hydrogeology J. 7, 341–354.

Medici, F., Rybach, L., 1995. Geothermal map of Switzerland (heat flow density). Matéraux pour la Géologie de la Suisse, Géophysique No. 30, Zürich, Switzerland.

Michalski, I., Soom, M., 1990. The Alpine thermo-tectonic evaluation of the Aar and Gotthard massifs, central Switzerland: fission-track ages on Zirkon and Apatite and K–Ar mica ages. Schweiz. Mineral. Petrogr. Mitt. 70, 373–387.

Niethammer, G., 1910. Die Wärmeleitung im Simplon. Eclogae Geol. Helv. 11, 96–120.

Pfiffner, O.A., Heitzmann, P., 1997. Geological interpretation of the seismic profiles of the central traverse (lines C1, C2 and C3 north). In: Pfiffner, et al. (Eds.), Results of NRP 20: Deep Structure of the Swiss Alps. Brinkhäuser Verlag, Basel, pp. 115–122.

Rybach, L., Čermák, V., 1982. Radio-active heat generation in rocks. Landolt-Börnstein, New Series, Group V (1a). Springer, Berlin, 353–371.

Rybach, L., Pfister, M., 1994. Temperature predictions and predictive temperatures in deep tunnels. Rock Mech. Rock Eng. 27 (2), 77–88.

Šafanda, J., 1999. Ground surface temperature as a function of the slope angle and slope orientation and its effect on surface temperature field. Tectonophysics 360, 367–375.

Schlatter, A., Marti, U., 1999. The new national height system (LHN95) of Switzerland. IUGG 99, Abstracts of general assembly, p. 417.

Signorelli S., 1999. Geothermische Messungen im NEAT-Schacht Sedrun und ihre Interpretation. Diploma Thesis, Institute of Geophysics, ETH Zürich, Switzerland.

Smith, L., Chapman, D.S., 1983. On the thermal effects of groundwater flow. 1. Regional scale systems. J. Geophys. Res. 88 (B1), 593–608.

Wegmann, M., Gudmundsson, G.H., Haeberli, W., 1998. Permafrost changes in rock walls and the retreat of Alpine glaciers: a thermal modelling approach. Permafrost Periglacial Proc. 9 (1), 23–33.

Wyder, R.F., Rybach, L., 1996. Determination of total porosity from litho-density log data (example from the NEAT-borehole SB3-Tujetseh). Schweiz. Mineral. Petrogr. Mitt. 76, 277–296.